Particle-balance models for pulsed sputtering magnetrons: The role of recycling

Jón Tómas Guðmundsson[1,2,3], Daniel Lundin[3], Michael A. Raadu[1], C. Huo[1], Nils Brenning[1] and Tiberu M. Minea[3]

[1] Department of Space and Plasma Physics, School of Electrical Engineering, KTH – Royal Institute of Technology, Stockholm, Sweden
[2] Science Institute, University of Iceland, Reykjavik, Iceland
[3] Laboratoire de Physique des Gaz et Plasmas - LPGP, UMR 8578 CNRS, Université Paris-Sud, 91405 Orsay Cedex, France

Plasma-Québec 2017, Montréal, Québec, Canada
May 18., 2017

Introduction

- Magnetron sputtering has been the workhorse of plasma based sputtering methods for almost five decades
- Magnetron sputtering discharges are widely used in thin film processing

- Applications include
  - thin films in integrated circuits
  - magnetic material
  - hard, protective, and wear resistant coatings
  - optical coatings
  - decorative coatings
  - low friction films

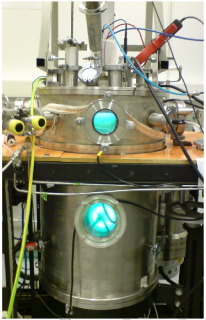

Introduction

- A magnet is placed at the back of the cathode target with the pole pieces at the center and perimeter
- The magnetic field confines the energetic electrons near the cathode, where they undergo numerous ionizing collisions before being lost to a grounded surface
- If the cathode plate is circular, the magnetic confinement is seen as a torus shaped plasma that hovers in front of the target

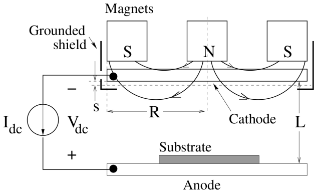

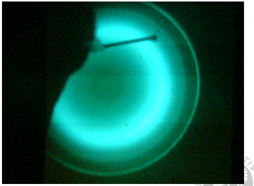

Introduction

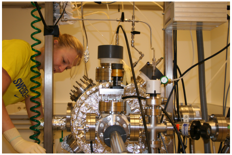

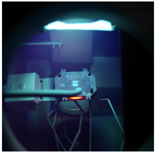

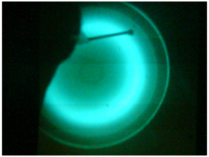

- Through the years there has been a continuous development of the magnetron sputtering processes to
  - increase the ionization of the sputtered vapor
  - improve target utilization
  - avoid target poisoning in reactive sputtering
- For many applications a high degree of ionization of the sputtered vapor is desired
  - controlled ion bombardment of the growing film
  - ion energy can be controlled by a negative bias applied to the substrate
  - collimation – enhanced step coverage

Introduction

- High ionization of sputtered material requires very high density plasma
- In a conventional dc magnetron sputtering discharge the power density (plasma density) is limited by the thermal load on the target
- High power pulsed magnetron sputtering (HPPMS)
- In a HiPIMS discharge a high power pulse is supplied for a short period
  - low frequency
  - low duty cycle
  - low average power

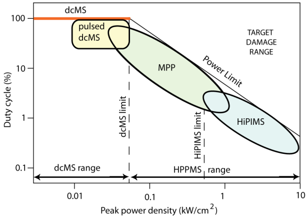

Gudmundsson et al. (2012), JVSTA **30** 030801

- Power density limits
  $p_t = 0.05$ kW/cm^2 dcMS limit
  $p_t = 0.5$ kW/cm^2 HiPIMS limit

Introduction

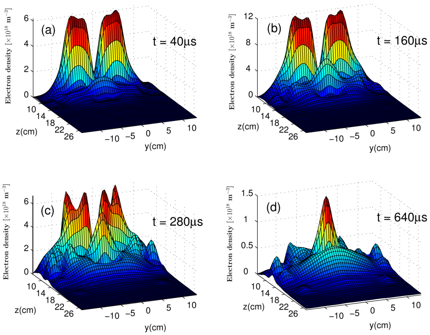

After Bohlmark et al. (2005), IEEE Trans. Plasma Sci. **33** 346

- Temporal and spatial variation of the electron density
- Ar discharge at 20 mTorr, Ti target, pulse length 100 μs
- The electron density in the substrate vicinity is of the order of $10^{18} - 10^{19}$ m^{-3} – ionization mean free path $\lambda_{\rm iz} \sim 1$ cm

Introduction

- Reactive sputtering, where metal targets are sputtered in a reactive gas atmosphere to deposit compound materials is of utmost importance in various technologies
- In reactive sputtering processes a reactive gas O_2, N_2, or CH_4 etc. is mixed to the noble working gas for oxide, nitride, or carbide deposition
- HiPIMS deposition generally gives denser, smoother films and higher crystallinity than dcMS grown films

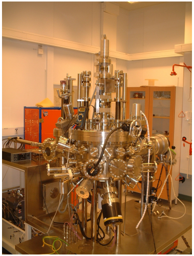

Helmersson et al. (2006) Thin Solid Films **513** 1

Magnus et al. (2012) IEEE EDL **33** 1045

Reactive HiPIMS - Applications

Application – Film Resistivity

- TiN as diffusion barriers for copper and aluminum interconnects
- HiPIMS deposited films have significantly lower resistivity than dcMS deposited films on SiO_2 at all growth temperatures due to reduced grain boundary scattering
- Thus, ultrathin continuous TiN films with superior electrical characteristics and high resistance towards oxidation can be obtained with HiPIMS at reduced temperatures

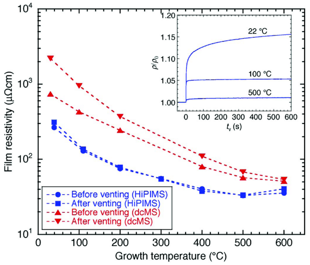

From Magnus et al. (2012) IEEE EDL **33** 1045

Application – Bragg mirror

- Multilayer structures containing a high-contrast (TiO_2/SiO_2) Bragg mirror
- fabricated on fused-silica substrates
  - reactive HiPIMS TiO_2 (88 nm)
  - reactive dcMS SiO_2 (163 nm)
  - capped with semitransparent gold
- Rutile TiO_2 (n = 2.59) and SiO_2 (n = 1.45) provide a large index contrast
- Smooth rutile TiO_2 films can be obtained by HiPIMS at relatively low growth temperatures, without post-annealing

Agnarsson et al. (2013) TSF **545** 445

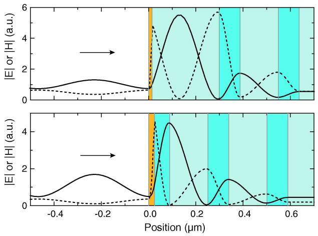

From Leosson et al. (2012) Opt. Lett. **37** 4026

Voltage - Current - Time characteristics

Non-reactive HiPIMS

HiPIMS - Voltage - Current - time

- In **non-reactive** discharge the current waveform shows an initial pressure dependent peak that is followed by a second phase that is power and material dependent
- The initial phase has a contribution from the working gas ions, whereas the later phase has a strong contribution from self-sputtering at high voltage

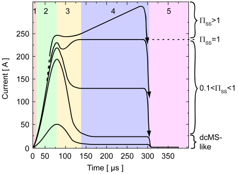

From Gudmundsson et al. (2012), JVSTA **30** 030801

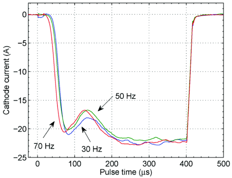

From Magnus et al. (2011) JAP **110** 083306

Ionization region model studies of non-reactive HiPIMS

Ionization region model non-reactive HiPIMS

- The ionization region model (IRM) was developed to improve the understanding of the plasma behaviour during a HiPIMS pulse and the afterglow
- The main feature of the model is that an ionization region (IR) is defined next to the race track
- The IR is defined as an annular cylinder with outer radii r_{c2}, inner radii r_{c1} and length $L = z_2 - z_1$, extends from z_1 to z_2 axially away from the target

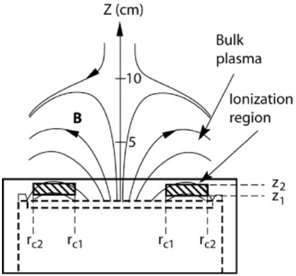

The definition of the volume covered by the IRM

From Raadu et al. (2011), PSST **20** 065007

Ionization region model non-reactive HiPIMS

- The temporal development is defined by a set of ordinary differential equations giving the first time derivatives of
  - the electron energy
  - the particle densities for all the particles
- The species assumed in the non-reactive-IRM are
  - electrons
  - argon atoms Ar($3s^2 3p^6$), warm argon atoms in the ground state Ar^W, hot argon atoms in the ground state Ar^H, Ar^m ($1s_5$ and $1s_3$) (11.6 eV), argon ions Ar^+ (15.76 eV)
  - titanium atoms Ti(a ^{3}F), titanium ions Ti^+ (6.83 eV), doubly ionized titanium ions Ti^{2+} (13.58 eV)
  - aluminium atoms Al($^2P_{1/2}$), aluminium ions Al^+ (5.99 eV), doubly ionized aluminium ions Al^{2+} (18.8 eV)

Detailed model description is given in Huo et al. (2017), JPD submitted 2017

Ionization region model non-reactive HiPIMS

- The model is constrained by experimental data input and fitted to reproduce the measured discharge current and voltage curves, $I_D(t)$ and $U_D(t)$, respectively
- Two model fitting parameters were found to be sufficient for a discharge with Al target
  - U_{IR} accounts for the power transfer to the electrons
  - β is the probability of back-attraction of ions to the target

From Huo et al. (2017), JPD submitted 2017

Experimental data from Anders et al. (2007) JAP **102** 113303

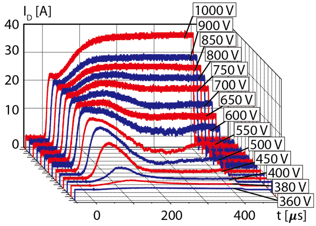

(a)

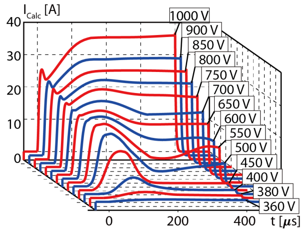

(b)

Ionization region model non-reactive HiPIMS

- A **non-reactive** discharge with Al target
- When the discharge is operated at 400 V the contributions of Al^+ and Ar^+-ions to the discharge current are very similar
- At 800 V Al^+-ions dominate the discharge current (**self-sputtering**) while the contribution of Ar^+ is below 10 % except at the initiation of the pulse

From Huo et al. (2017), JPD submitted 2017

Experimental data from Anders et al. (2007) JAP **102** 113303

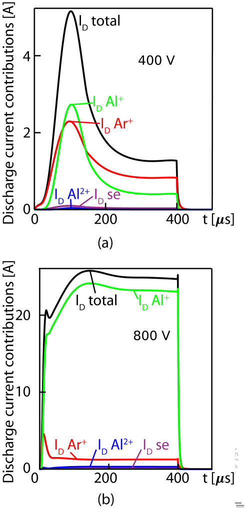

Ionization region model non-reactive HiPIMS

- A **non-reactive** discharge with Ti target
- The contributions to the discharge current for two cases, weak (180 Gauss) and strong (380 Gauss) magnetic field, at 75 Hz pulse frequency
- Stronger magnetic field leads to a higher discharge current
- Higher magnetic field strength leads to higher relative contribution of Ti^{2+} while it lowers the relative contribution of Ti^{+}

From Huo et al. (2017), JPD submitted 2017

Experimental data from Bradley et al. (2015) JPD **48** 215202

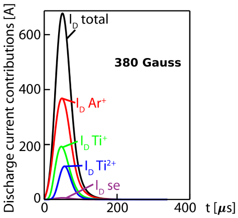

(a)

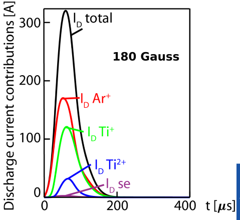

(b)

Ionization region model non-reactive HiPIMS

- A primary current I_{prim} is defined as ions of the working gas, here Ar^+, that are ionized for the first time and then drawn to the target
- This is the dominating current in dc magnetron sputtering discharges
- This current has a critical upper limit

$$I_{\mathrm{crit}} = S_{\mathrm{RT}} e p_{\mathrm{g}} \sqrt{\frac{1}{2\pi m_{\mathrm{g}} k_{\mathrm{B}} T_{\mathrm{g}}}} = S_{\mathrm{RT}} e n_{\mathrm{g}} \sqrt{\frac{k_{\mathrm{B}} T_{\mathrm{g}}}{2\pi m_{\mathrm{g}}}}$$

- Discharge currents I_{D} above I_{crit} are only possible if there is some kind of recycling of atoms that leave the target, become subsequently ionized and then are drawn back to the target

Anders et al. (2012), JPD **45** 012003

Huo et al. (2014), PSST **23** 025017

Ionization region model non-reactive HiPIMS

- For the Al target the critical current is $I_{\rm crit} \approx 7$ A
- The experiment is operated from far below $I_{\rm crit}$ to high above it, up to 36 A.
- With increasing current $I_{\rm prim}$ gradually becomes a very small fraction of the total discharge current $I_{\rm D}$
- The current becomes mainly carried by singly charged $\rm Al^+$ ions, meaning that the current $I_{\rm SS-recycle}$ or **self-sputter recycling** dominates

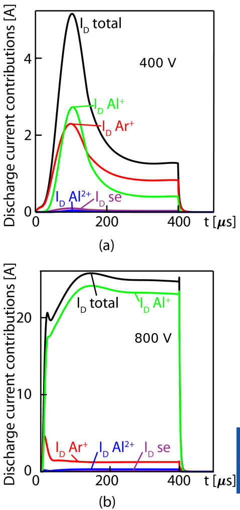

From Huo et al. (2017), JPD submitted 2017

Experimental data from Anders et al. (2007) JAP **102** 113303

Ionization region model non-reactive HiPIMS

- The discharge with the Ti target is operated with peak current far above the critical current of $I_{\mathrm{crit}} \approx 19$ A
- This discharge shows close to a 50/50 combination of **self-sputter recycling** $I_{\mathrm{SS-recycle}}$ and **working gas-recycling** $I_{\mathrm{gas-recycle}}$

From Huo et al. (2017), JPD submitted 2017

Experimental data from Bradley et al. (2015) JPD **48** 215202

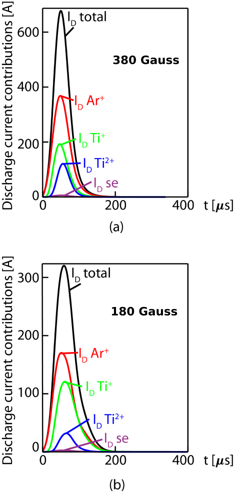

Ionization region model non-reactive HiPIMS

- Recall that singly charged metal ions cannot create the secondary electrons – for metal self-sputtering (γ_{SE} is practically zero)
- The first ionization energies of many metals are insufficient to overcome the workfunction of the target material
- For the discharge with Al target operated at high voltage, self-sputter dominated, the effective secondary electron emission is close to zero

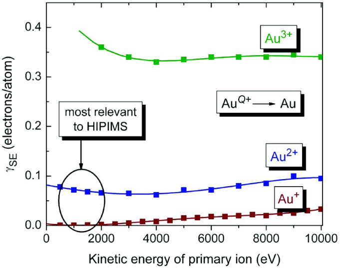

From Anders (2008) APL **92** 201501

Ionization region model non-reactive HiPIMS

- The power transfer to the electrons is given by

$$P_{\rm e} = P_{\rm SH} + P_{\rm Ohm} = I_{\rm e,SH}\left(U_{\rm D} - U_{\rm IR}\right) + \frac{I_{\rm D} U_{\rm IR}}{2}$$

where

$$P_{\rm SH} = I_{\rm e,SH} U_{\rm SH} = \left(I_{\rm Ar^+} \gamma_{\rm Ar^+,eff} + \frac{1}{2} I_{\rm M^{2+}} \gamma_{\rm M^{2+},eff} \right) U_{\rm SH}$$

and

$$P_{\rm Ohm} = I_{\rm e,IR} U_{\rm IR} = \left\langle \frac{J_{\rm e}}{J_{\rm D}} \right\rangle I_{\rm D} U_{\rm IR}$$

- Then $I_{\rm e,SH} \sim \gamma_{\rm SE} \epsilon_{\rm e} m(1-r) I_{\rm D} \sim 0.05 I_{\rm D}$ and $I_{\rm e,SH} \ll I_{\rm D}/2$ so that

$$I_{\rm e,SH} \ll I_{\rm D}/2$$

and Ohmic heating is more efficient

Ionization region model non-reactive HiPIMS

- For the Al target, the fraction of the total electron heating that is attributable to Ohmic heating is found in the range of 0.87 (360 V) to 0.99 (1000 V).
- The domination of Al^{+}-ions, which have zero secondary electron emission yield, has the consequence that there is negligible sheath energization
- The ionization threshold for twice ionized Al^{2+}, 18.8 eV, is so high that few such ions are produced

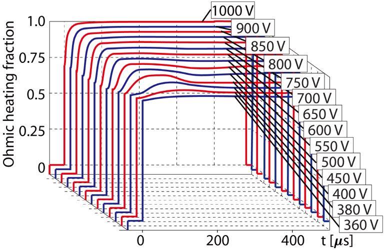

From Huo et al. (2017), JPD submitted 2017

Ionization region model non-reactive HiPIMS

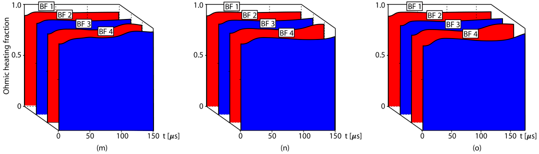

- For the discharge with Ti target more Ar^{+}-ions contribute to the current and the ionization degree of Ti^{2+} is more than order of magnitude larger than the ionization degree of Al^{2+}, so there are more secondary electrons
- The fraction of the total electron heating that is attributable to Ohmic heating is about 0.92
- Decreasing the magnetic field strength (BF1 to BF4) slightly reduces the Ohmic heating fraction

From Huo et al. (2017), JPD submitted 2017

Ionization region model non-reactive HiPIMS

- The model results show that for an argon discharge with Al target the contribution of Al^{+}-ions is over 90 % at 800 V, while Al^{+}-ions and Ar^{+}-ions contribute roughly equally to the discharge current at 400 V
- For high currents the discharge with Al target develops almost pure **self-sputter recycling**, while the discharge with Ti target exhibits close to a 50/50 combination of **self-sputter recycling** and **working gas-recycling**
- For a Ti target, a self-sputter yield significantly below unity makes working gas-recycling necessary at high currents.
- The model results show that Al^{2+}-ions contribute negligibly, while Ti^{2+}-ions effectively contribute to the production of secondary electrons
- The fraction of the total electron heating that is attributable to Ohmic heating is over 90 %

Voltage - Current - Time characteristics

Reactive HiPIMS

HiPIMS - Voltage - Current - time

- During **reactive sputtering**, a reactive gas is added to the inert working gas
- The current waveform in the reactive Ar/N_2 HiPIMS discharge with Ti target is highly dependent on the pulse repetition frequency
- N_2 addition changes the plasma composition and the target condition can also change due to the formation of a compound on its surface

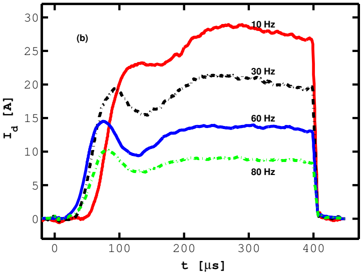

After Magnus et al. (2011) JAP **110** 083306

HiPIMS - Voltage - Current - time

- Similarly for the Ar/O_2 discharge, the current waveform is highly dependent on the repetition frequency and applied voltage which is linked to oxide formation on the target
- The current is found to increase significantly as the frequency is lowered

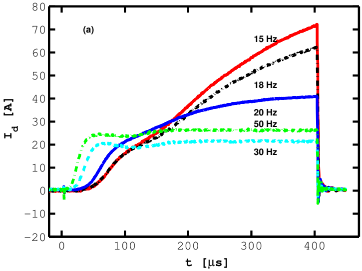

After Magnus et al. (2012), JVSTA **30** 050601

HiPIMS - Voltage - Current - time

- As the oxygen flow is increased a transition to oxide mode is observed

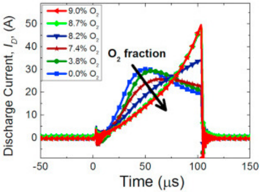

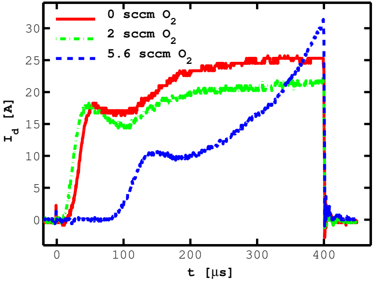

The current waveforms for an Ar/O_2 discharge with a V target where the oxygen flow rate is varied

From Aijaz et al. (2016) Solar Energy Materials and Solar Cells **149** 137

The current waveforms for an Ar/O_2 discharge with a Ti target where the oxygen flow rate is varied – 600 V, 50 Hz and 0.6 Pa

From Gudmundsson et al. (2013), ISSP 2013, p. 192

Gudmundsson (2016) Plasma Phys. Contr. Fus. **58** 014002

HiPIMS - Voltage - Current - time

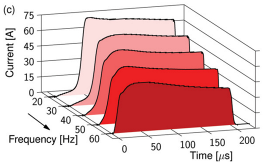

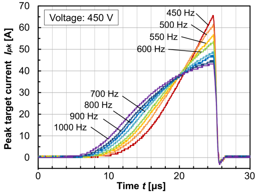

- Similar behaviour has been reported for various target and reactive gas combinations
  - The current increases with decreased repetition frequency
  - The current waveform maintains its shape for Ar/O_2 discharge with Nb target

  From Hála et al. (2012), JPD **45** 055204
  - The current waveform becomes distinctly triangular for Ar/N_2 discharge with Hf target

  From Shimizu et al. (2016), JPD **49** 065202

HiPIMS - Voltage - Current - time

- The current increases with increased partial pressure of the reactive gas
  - The current waveform becomes distinctly triangular for Ar/N_2 discharge with Al target

    From Moreira et al. (2015), JVSTA **33** 021518
  - The current waveform maintains its shape for Ar/O_2 discharge with Nb target

    From Hála et al. (2012), JPD **45** 055204

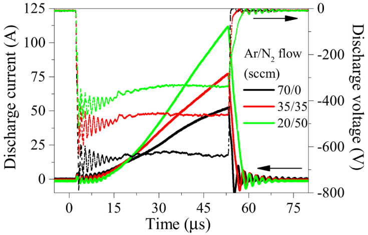

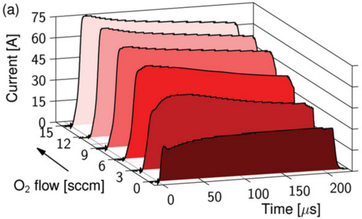

Ionization region model studies of reactive HiPIMS

Ionization region model studies of reactive HiPIMS

- The species assumed in the reactive-IRM are
  - electrons
  - argon atoms Ar($3s^2 3p^6$), warm argon atoms in the ground state Ar^W, hot argon atoms in the ground state Ar^H, Ar^m ($1s_5$ and $1s_3$) (11.6 eV), argon ions Ar^+ (15.76 eV)
  - titanium atoms Ti(a ^{3}F), titanium ions Ti^+ (6.83 eV), doubly ionized titanium ions Ti^{2+} (13.58 eV)
  - oxygen molecule in the ground state $O_2(X^3\Sigma_g^-)$, the metastable oxygen molecules $O_2(a^1\Delta_g)$ (0.98 eV) and $O_2(b^1\Sigma_g)$ (1.627 eV), the oxygen atom in the ground state O(^{3}P), the metastable oxygen atom O(^{1}D) (1.96 eV), the positive ions O_2^+ (12.61 eV) and O^+ (13.62 eV), and the negative ion O^-

Oxygen chemistry based on Toneli et al. (2015) J. Phys. D. **48** 325202

Ionization region model studies of reactive HiPIMS

- The sputter yield for the various bombarding ions was calculated by TRIDYN for
  - **Metal mode** – Ti target
  - **Poisoned mode** – TiO_2 target
- The yields correspond to the extreme cases of either clean Ti surface and a surface completely oxidized (TiO_2 surface)
- The sputter yield is much lower for poisoned target

The sputter yield data is from Tomas Kubart, Uppsala University

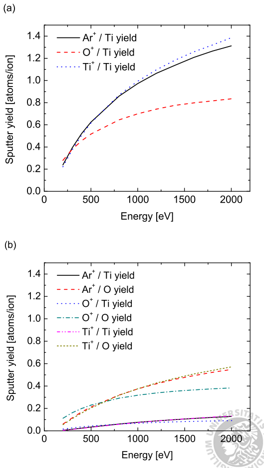

Ionization region model studies of reactive HiPIMS

- The model is applied to explore Ar/O_2 discharge with Ti target in both metal mode and oxide (poisoned) mode
- The IRM is a semi-empirical model in the sense that it uses a measured discharge voltage and current waveforms as a main input parameter
- For this study we use the measured curve for Ar/O_2 with Ti target at 50 Hz for metal mode and at 15 Hz for poisoned mode

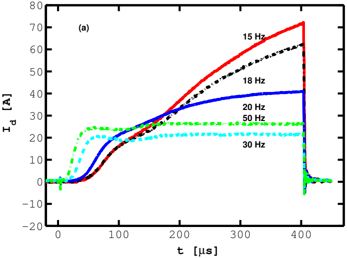

After Magnus et al. (2012), JVSTA **30** 050601

Ionization region model studies of reactive HiPIMS

- The gas rarefaction is observed for the argon atoms but is more significant for the O_2 molecule
- The density of Ti atoms is higher than the O_2 density
- The atomic oxygen density of is over one order of magnitude lower than the molecular oxygen density – the dissociation fraction is low

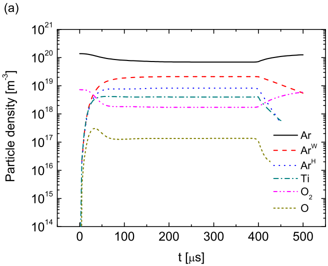

The temporal evolution of the neutral species with **5 % oxygen partial flow** rate for Ar/O_2 discharge with Ti target in **metal mode**.

Gudmundsson et al. (2016), PSST, 25(6) 065004

Ionization region model studies of reactive HiPIMS

- Gas rarefaction is observed for both argon atoms and O_2 molecules
- The density of Ti atoms is lower than both the O_2 density and atomic oxygen density
- The atomic oxygen density is higher than the O_2 density towards the end of the pulse

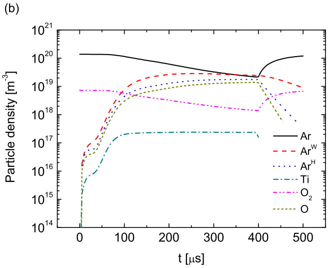

The temporal evolution of the neutral species with **5 % oxygen partial flow** rate for Ar/O_2 discharge with Ti target in **poisoned mode**.

Gudmundsson et al. (2016), PSST, 25(6) 065004

Ionization region model studies of reactive HiPIMS

- The increase in the atomic oxygen in the ground state is due to:
    - sputtering of $O(^3P)$ from the partially to fully oxidized target (dominates)
    - electron impact de-excitation of $O(^1D)$
    - electron impact dissociation of the O_2 ground state molecule

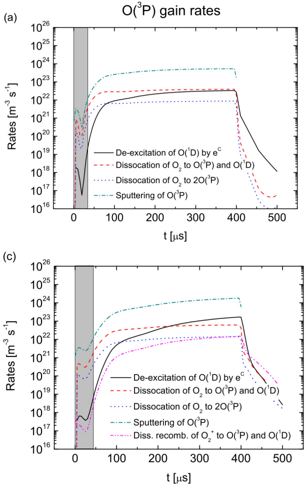

The temporal evolution of the neutral species with **5 % oxygen partial flow** rate for Ar/O_2 discharge with Ti target in **transition mode** and **poisoned mode**.

Lundin et al. (2017), JAP, 121(17) 171917

Ionization region model studies of reactive HiPIMS

- Ar^+ and Ti^+-ions dominate the discharge
- Ti^{2+}-ions follow by roughly an order of magnitude lower density
- The O_2^+ and O^+-ion density is much lower

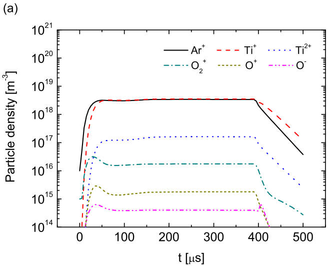

The temporal evolution of the neutral species with **5 % oxygen partial flow** rate for Ar/O_2 discharge with Ti target in **metal mode**.

Gudmundsson et al. (2016), PSST, 25(6) 065004

Ionization region model studies of reactive HiPIMS

- Ar^+-ions dominate the discharge
- Ti^+, O^+, have very similar density, but the temporal variation is different, and the O_2^+ density is slightly lower
- The Ti^{2+}-ion density increases fast with time and overcomes the O_2^+ density towards the end of the pulse

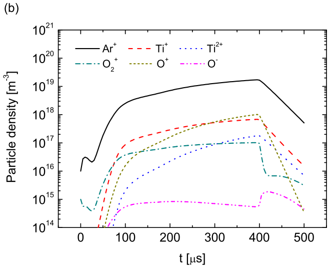

The temporal evolution of the neutral species with **5 % oxygen partial flow** rate for Ar/O_2 discharge with Ti target in **poisoned mode**.

Gudmundsson et al. (2016), PSST, 25(6) 065004

Ionization region model studies of reactive HiPIMS

- Ar^+ and Ti^+-ions contribute most significantly to the discharge current at the cathode target surface – almost equal contribution
- $I_{crit} \approx 5$ A

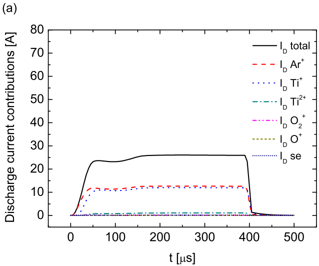

The temporal evolution of the neutral species with **5 % oxygen partial flow** rate for Ar/O_2 discharge with Ti target in **metal mode**.

Gudmundsson et al. (2016), PSST, 25(6) 065004

Ionization region model studies of reactive HiPIMS

- Ar^+ contribute most significantly to the discharge current – almost solely – at the cathode target surface
- The contribution of secondary electron emission is very small
- $I_{\rm crit} \approx 5$ A

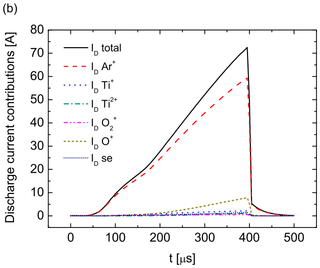

The temporal evolution of the neutral species with **5 % oxygen partial flow** rate for Ar/O_2 discharge with Ti target in **poisoned mode**.

Gudmundsson et al. (2016), PSST, 25(6) 065004

Ionization region model studies of reactive HiPIMS

- Towards the end of the pulse more than half of the Ar^+-ions are created from argon atoms that come from the target
  - a hot component Ar^H that returns from the target with a typical sputter energy of a few electron volts
  - a warm component Ar^W, embedded in the target at the ion impact, and then return to the surface and finally leaves with the target temperature, at most 0.1 eV

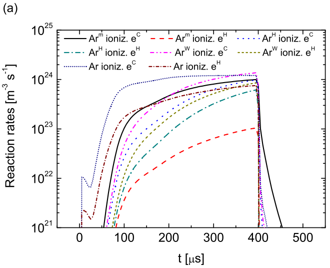

The temporal variations of the reaction rates for electron impact ionization of the argon atoms (ground state plus metastable) in **poisoned mode**.

Gudmundsson et al. (2016), PSST, 25(6) 065004

Ionization region model studies of reactive HiPIMS

- The sum of the ionization rates for the e^C plus the e^H populations, and that for the e^H electron population alone
- Here both the metal and the poisoned mode are shown
- The hot electron reactions are more important in the poisoned mode

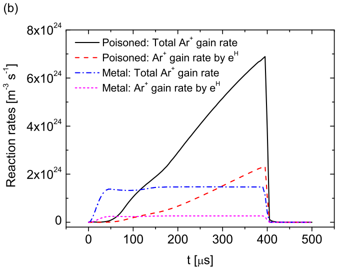

The temporal variations of the reaction rates for electron impact ionization of the argon atoms (ground state plus metastable).

Gudmundsson et al. (2016), PSST, 25(6) 065004

Ionization region model studies of reactive HiPIMS

- Recycling of atoms coming from the target and then ionized are required for the current generation in both modes of operation
- In the metal mode **self-sputter recycling** dominates and in the poisoned mode **working gas recycling** dominates
- The dominating type of recycling determines the discharge current waveform

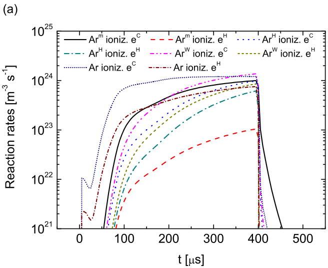

The temporal variations of the reaction rates for electron impact ionization of the argon atoms (ground state plus metastable) in poisoned mode.

Gudmundsson et al. (2016), PSST, 25(6) 065004

Ionization region model studies of reactive HiPIMS

- In the metal mode sheath energization was found to be only 10 %
  - same range as the results reported earlier for an Al target

    Huo et al. (2013), PSST **22**(4) 045005

  the dominating electron heating mechanism is Ohmic heating
- For the poisoned mode the sheath energization was 30 %, with a rising trend, at the end of the pulse
- This is due to the secondary electron emission
  - In the poisoned mode essentially all the ions (mainly Ar^+, but also O^+ and Ti^{2+} towards the end of the pulse) contribute to the secondary electron emission
  - In the metal mode only half of the ions contribute to the secondary electron emission (Ar^+) while the other half does not contribute at all ($\gamma_{Ti^+} = 0.0$)

Summary

Summary

- An ionization region model was used to explore the plasma composition during the high power pulse
- Comparison was made between the metal mode and the poisoned mode
  - In metal mode Ar^+ and Ti^+-ions dominate the discharge and are of the same order of magnitude
  - In poisoned mode Ar^+-ions dominate the discharge and two orders of magnitude lower, Ti^+, O^+, have very similar density, with the O_2^+ density slightly lower
  - In the metal mode Ar^+ and Ti^+-ions contribute most significantly to the discharge current while in poisoned mode Ar^+ dominate
- In the metal mode self-sputter recycling dominates and in the poisoned mode working gas recycling dominates – the dominating type of recycling determines the discharge current waveform

Thank you for your attention

The slides can be downloaded at

`http://langmuir.raunvis.hi.is/~tumi/ranns.html`

- We got help with the sputtering yields from
  - Dr. Tomas Kubart, Uppsala University, Uppsala, Sweden
- and the project is funded by
  - Icelandic Research Fund Grant No. 130029
  - Swedish Government Agency for Innovation Systems (VINNOVA) contract no. 2014-04876

References

Agnarsson, B., F. Magnus, T. K. Tryggvason, A. S. Ingason, K. Leosson, S. Olafsson, and J. T. Gudmundsson (2013). Rutile TiO_2 thin films grown by reactive high power impulse magnetron sputtering. *Thin Solid Films 545*, 445–450.

Aijaz, A., Y.-X. Ji, J. Montero, G. A. Niklasson, C. G. Granqvist, and T. Kubart (2016). Low-temperature synthesis of thermochromic vanadium dioxide thin films by reactive high power impulse magnetron sputtering. *Solar Energy Materials and Solar Cells 149*, 137–144.

Aiempanakit, M., A. Aijaz, D. Lundin, U. Helmersson, and T. Kubart (2013). Understanding the discharge current behavior in reactive high power impulse magnetron sputtering of oxides. *Journal of Applied Physics 113*(13), 133302.

Anders, A., J. Andersson, and A. Ehiasarian (2007). High power impulse magnetron sputtering: Current-voltage-time characteristics indicate the onset of sustained self-sputtering. *Journal of Applied Physics 102*(11), 113303.

Anders, A. (2008). Self-sputtering runaway in high power impulse magnetron sputtering: The role of secondary electrons and multiply charged metal ions. *Applied Physics Letters 92*(20), 201501.

Anders, A., J. Čapek, M. Hála, and L. Martinu (2012). The 'recycling trap': a generalized explanation of discharge runaway in high-power impulse magnetron sputtering. *Journal of Physics D: Applied Physics 45*(1), 012003.

Bohlmark, J., J. T. Gudmundsson, J. Alami, M. Lattemann, and U. Helmersson (2005). Spatial electron density distribution in a high-power pulsed magnetron discharge. *IEEE Transactions on Plasma Science 33*(2), 346–347.

Bradley, J. W., A. Mishra, and P. J. Kelly (2015). The effect of changing the magnetic field strength on HiPIMS deposition rates. *Journal of Physics D: Applied Physics 48*(21), 215202.

Gudmundsson, J. T. (2016). On reactive high power impulse magnetron sputtering. *Plasma Physics and Controlled Fusion 58*(1), 014002.

Gudmundsson, J. T., N. Brenning, D. Lundin, and U. Helmersson (2012). The high power impulse magnetron sputtering discharge. *Journal of Vacuum Science and Technology A 30*(3), 030801.

References

Gudmundsson, J. T., F. Magnus, T. K. Tryggvason, S. Shayestehaminzadeh, O. B. Sveinsson, and S. Olafsson (2013). Reactive high power impulse magnetron sputtering. In *Proceedings of the XII International Symposium on Sputtering and Plasma Processes (ISSP 2013)*, pp. 192–194.

Gudmundsson, J. T., D. Lundin, N. Brenning, M. A. Raadu, C. Huo, and T. M. Minea (2016). An ionization region model of the reactive Ar/O_2 high power impulse magnetron sputtering discharge. *Plasma Sources Science and Technology 25*(6), 065004.

Hála, M., J. Čapek, O. Zabeida, J. E. Klemberg-Sapieha, and L. Martinu (2012). Hysteresis - free deposition of niobium oxide films by HiPIMS using different pulse management strategies. *Journal of Physics D: Applied Physics 45*(5), 055204.

Helmersson, U., M. Lattemann, J. Bohlmark, A. P. Ehiasarian, and J. T. Gudmundsson (2006). Ionized physical vapor deposition (IPVD): A review of technology and applications. *Thin Solid Films 513*(1-2), 1–24.

Huo, C., D. Lundin, M. A. Raadu, A. Anders, J. T. Gudmundsson, and N. Brenning (2013). On sheath energization and ohmic heating in sputtering magnetrons. *Plasma Sources Science and Technology 22*(4), 045005.

Huo, C., D. Lundin, M. A. Raadu, A. Anders, J. T. Gudmundsson, and N. Brenning (2014). On the road to self-sputtering in high power impulse magnetron sputtering: particle balance and discharge characteristics. *Plasma Sources Science and Technology 23*(2), 025017.

Huo, C., D. Lundin, J. T. Gudmundsson, M. A. Raadu, J. W. Bradley, and N. Brenning (submitted 2017). Particle-balance models for pulsed sputtering magnetrons. *Journal of Physics D: Applied Physics*.

Lundin, D., J. T. Gudmundsson, N. Brenning, M. A. Raadu, and T. M. Minea (2017). A study of the oxygen dynamics in a reactive Ar/O_2 high power impulse magnetron sputtering discharge using an ionization region model. *Journal of Applied Physics 121*(17), 171917.

Leosson, K., S. Shayestehaminzadeh, T. K. Tryggvason, A. Kossoy, B. Agnarsson, F. Magnus, S. Olafsson, J. T. Gudmundsson, E. B. Magnusson, and I. A. Shelykh (2012). Comparing resonant photon tunneling via cavity modes and Tamm plasmon polariton modes in metal-coated Bragg mirrors. *Optics Letters 37*(19), 4026–4028.

References

Magnus, F., A. S. Ingason, S. Olafsson, and J. T. Gudmundsson (2012). Nucleation and resistivity of ultrathin TiN films grown by high power impulse magnetron sputtering. *IEEE Electron Device Letters 33*(7), 1045 – 1047.

Magnus, F., O. B. Sveinsson, S. Olafsson, and J. T. Gudmundsson (2011). Current-voltage-time characteristics of the reactive Ar/N_2 high power impulse magnetron sputtering discharge. *Journal of Applied Physics 110*(8), 083306.

Magnus, F., T. K. Tryggvason, S. Olafsson, and J. T. Gudmundsson (2012). Current-voltage-time characteristics of the reactive Ar/O_2 high power impulse magnetron sputtering discharge. *Journal of Vacuum Science and Technology A 30*(5), 050601.

Moreira, M. A., T. Törndahl, I. Katardjiev, and T. Kubart (2015). Deposition of highly textured AlN thin films by reactive high power impulse magnetron sputtering. *Journal of Vacuum Science and Technology A 33*(2), 021518.

Raadu, M. A., I. Axnäs, J. T. Gudmundsson, C. Huo, and N. Brenning (2011). An ionization region model for high power impulse magnetron sputtering discharges. *Plasma Sources Science and Technology 20*(6), 065007.

Shimizu, T., M. Villamayor, D. Lundin, and U. Helmersson (2015). Process stabilization by peak current regulation in reactive high-power impulse magnetron sputtering of hafnium nitride. *Journal of Physics D: Applied Physics 49*(6), 065202.

Toneli, D. A., R. S. Pessoa, M. Roberto, and J. T. Gudmundsson (2015). On the formation and annihilation of the singlet molecular metastables in an oxygen discharge. *Journal of Physics D: Applied Physics 48*(32), 325202.